efficiency will be equal 64.9%. The time of PCM charging equals 8 hours is assumed. Now, since the mass flow rate of HTF provides the required thermal energy for melting of PCM, the storage thermal energy of PCM increases the temperature of HTF from $35^{\circ}C$ to $50^{\circ}C$ during the night. Also, the discharging time of PCM based on the time of charging and mass flow rate of HTF during the night must be considered. As shown in figure 4, it is clearly that the reaching time of HTF to $50^{\circ}C$ temperature is equal to 400 minutes after operating the thermal discharge. The period of discharging time of PCM and attaining / reaching time to the temperature of $50^{\circ}C$ were shown in figure 4.

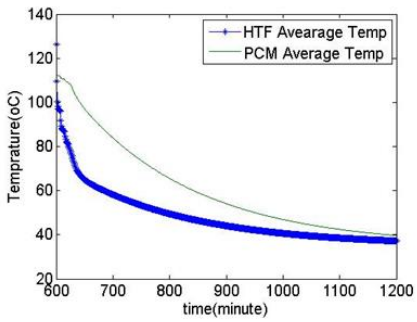

Figure 4. Variation of HTF and PCM temperature versus time.

4. CONCLUSIONS

In the first step, the thermodynamic modeling and the exergy analysis in the lithium-bromide absorption chiller cycle has been carried out and then, the principal parameters of cycle have been optimized by a genetic algorithm. In the second step, the type of collector and the mass of phase changing material have been assigned. Finally, by focusing on the time of using absorption chiller, the temperature changes of HTF and PCM are being discussed along the time. It should be noted that during the discharging time, the storage thermal energy of PCM transmits to HTF. It is clearly shown that attaining/reaching time of HTF to $50^{\circ}C$ is equal to 400 minutes after the operating thermal discharge.

REFERENCES

[1] Sidiras D.K., Koukios E.G. (2003). The solar thermal market in Greece-review and perspectives, *Renewable and Sustainable Energy Reviews*, Vol. 7, pp. 397-418.

[2] Schlaich J., Bergermann R., Schiel W. (2005). Design of commercial solar updraft tower systems- utilization of solar induced convective flows for power generation, *Journal of Solar Energy Engineering*, Vol. 1, pp. 117-124.

[3] Misra R.D., Sahoo P.K., Gupta A. (2005). Thermoeconomic optimization of a single effect vapor absorption refrigeration system, *Journal of Energy Resources Technology*, Vol. 26, pp. 158-169.

[4] Li Z.F., Sumathy K. (2001). Simulation of a solar absorption air conditioning system, *Energy Conversion and Management*, Vol. 42, No. 3, pp. 313-327.

[5] Li Z.F., Sumathy K. (2001). Experimental studies on a solar powered air conditioning system with partitioned hot water storage tank, *Solar Energy*, Vol. 71, No. 5, pp. 285-297.

[6] Atmaca I., Yigit A. (2003). Simulation of solar-powered absorption cooling system, *Renewable Energy*, Vol. 28, No. 8, pp. 1277-1293.

[7] Sayegh M.A. (2007). The solar contribution to air conditioning systems for residential buildings, *Desalination*, Vol. 29, pp. 171-176.

[8] Talbi M.M., Agnew B. (2000). Exergy analysis: an absorption refrigerator using lithium bromide and water as the working fluids, *Applied Thermal Engineering*, Vol. 20, pp. 619-630.

[9] Şencan A., Yakut K.A., Soteris A. (2005). Exergy analysis of lithium bromide/water absorption systems, *Renewable Energy*, Vol. 30, pp. 645- 657.

[10] Infante Ferreira C.A., Kim D.S. (2014). Techno-economic review of solar cooling technologies based on location-specific data, *Int. J. Refrig*., Vol. 39, pp. 23–27.

[11] Sayadi Z., Thameur N.B., Bourouis M., Bellagi A. (2013). Performance optimization of solar driven small-cooled absorption–diffusion chiller working with light hydrocarbons, *Energy Conversion and Management*, Vol. 74, pp. 299–307.

[12] Falahatkar A., Akhavan H. (2014). Design and simulation of a single effect LiBr–H_2O absorption chiller for a building in Tehran, *Energy Journal of Iran*, Vol. 14, pp. 37–46.

[13] Mirandola A., Lorenzini E. (2016). Energy, environment and climate: from the past to the future, *International Journal of Heat and Technology*, Vol. 34, No. 2, pp. 159-164. DOI: 10.18280/ijht.340201

[14] Casano G., Piva S. (2015). Parametric analysis of a PCM energy storage system, *International Journal of Heat and Technology*, Vol. 33, No. 4, pp. 61-68. DOI: 10.18280/ijht.330408

SYMBOLES

COP	Coefficient of performance (-)
E	Exergy, ($kJkg^{-1}$)
E_D	Exergy destruction, ($kJkg^{-1}$)
F_R	collector heat removal factor
G	monthly solar radiation on the horizontal surface, (Wm^2)
h	Enthalpy, ($kJkg^{-1}$)
U_L	collector overall heat loss coefficient, (Wm^{-2})
α	absorption coefficient of plate
τ	transmission coefficient of glazing
$\eta_{collector}$	collector efficiency, (%)
$q_{collector}$	collector heat output, (W)